

## Accepted Manuscript

Title: Tungstenocene-grafted silica catalysts for the selective epoxidation of alkenes

Authors: Chiara Bisio, Alessandro Gallo, Rinaldo Psaro, Cristina Tiozzo, Matteo Guidotti, Fabio Carniato



PII: S0926-860X(19)30240-6  
DOI: <https://doi.org/10.1016/j.apcata.2019.05.027>  
Reference: APCATA 17093

To appear in: *Applied Catalysis A: General*

Received date: 16 December 2018  
Revised date: 12 May 2019  
Accepted date: 24 May 2019

Please cite this article as: Bisio C, Gallo A, Psaro R, Tiozzo C, Guidotti M, Carniato F, Tungstenocene-grafted silica catalysts for the selective epoxidation of alkenes, *Applied Catalysis A, General* (2019), <https://doi.org/10.1016/j.apcata.2019.05.027>

This is a PDF file of an unedited manuscript that has been accepted for publication. As a service to our customers we are providing this early version of the manuscript. The manuscript will undergo copyediting, typesetting, and review of the resulting proof before it is published in its final form. Please note that during the production process errors may be discovered which could affect the content, and all legal disclaimers that apply to the journal pertain.

# Tungstenocene-grafted silica catalysts for the selective epoxidation of alkenes

Chiara Bisio,<sup>a,b</sup> Alessandro Gallo,<sup>\*c,d</sup> Rinaldo Psaro,<sup>a</sup>

Cristina Tiozzo<sup>a</sup>, Matteo Guidotti<sup>\*a</sup> and Fabio Carniato<sup>b</sup>

<sup>a</sup> *CNR-Institute of Molecular Sciences and Technologies, Via C. Golgi 19, Milan, Italy*

<sup>b</sup> *University of Eastern Piedmont "A.Avogadro", Viale T. Michel 11, Alessandria, Italy*

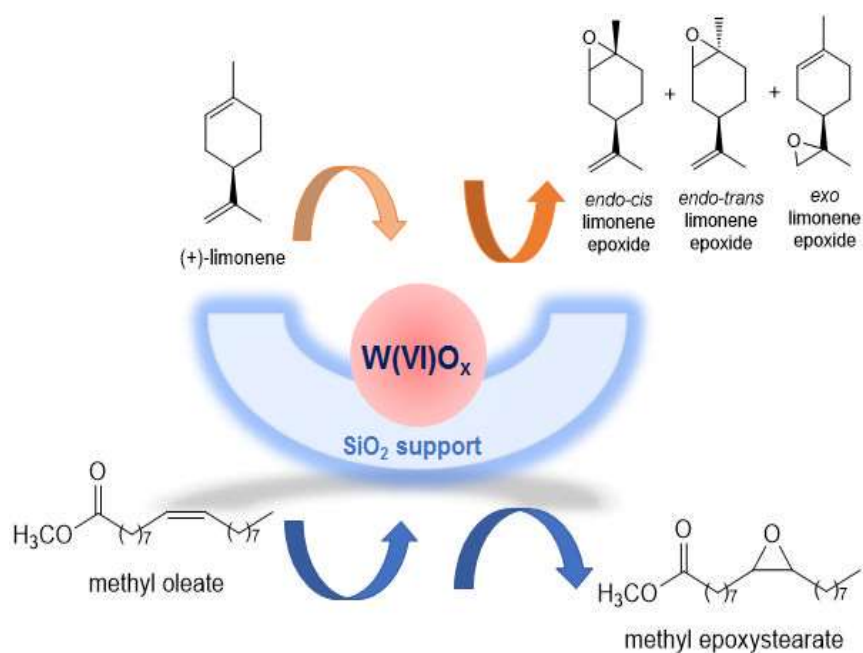
<sup>c</sup> *SUNCAT Center for Interface Science and Catalysis, Department of Chemical Engineering, Stanford University, Stanford, California 94305, United States*

<sup>d</sup> *SUNCAT Center for Interface Science and Catalysis, SLAC National Accelerator Laboratory, Menlo Park, California 94025, United States*

(\*) corresponding authors: [m.guidotti@istm.cnr.it](mailto:m.guidotti@istm.cnr.it) ; [agallo@slac.stanford.edu](mailto:agallo@slac.stanford.edu)

*dedicated to Prof. Guido Busca on the occasion of his 65th birthday*

Graphical Abstract



## Highlights

- - Tungsten(VI)-silica heterogeneous catalysts for the epoxidation of alkenes
- - Two novel preparation approaches from tungstenocene(IV) dichloride and commercial silica
- - Extended physico-chemical characterisation of the surface W(IV) species
- - Good performance as catalysts for the epoxidation of limonene and methyl oleate with  $H_2O_2$
- - Promising robustness of the tungsten-grafted silica catalysts against metal leaching

## ABSTRACT

Tungstenocene(IV) dichloride was successfully deposited and grafted on the surface of a commercially-available non-ordered silica support via either a liquid-phase or a dry impregnation approach. After a high-temperature calcination step, two W(VI)-grafted silica catalysts, with a metal loading around 1.2-1.7 wt.%, were obtained. They were fully characterized by physisorption and spectroscopic techniques, which evidenced well-dispersed tungsten oxide polyoxo cluster sites, for the catalyst prepared via liquid-phase grafting, and evenly dispersed larger monoclinic tungsten(VI) oxide aggregates, for the catalyst prepared via dry impregnation, respectively. Both  $W/SiO_2$  solids showed moderate to good conversion values in the epoxidation of (*R*)-(+)-limonene and methyl oleate (up to 68%), in the presence of aqueous hydrogen peroxide, with good selectivity to the desired epoxides (63% and 78%, respectively). The heterogeneous

character of the most interesting W/SiO<sub>2</sub> catalyst prepared via dry impregnation was confirmed by a hot centrifugation test and by an extended recovery and reuse of the solid in six catalytic runs.

**Keywords:** Epoxidation; hydrogen peroxide; heterogeneous catalyst; tungsten-silica catalyst; tungstenocene dichloride; alkenes; XAS.

## INTRODUCTION

In the panorama of single-site heterogeneous catalysts, the generation of active metal sites on the surface of high-surface area inorganic oxides can be achieved by covalently grafting organometallic precursors onto the solid support and by subsequent thermal treatment, in order to obtain a stable, active, easy-to-handle and recyclable system [1,2]. The grafting approach allows the synthetic chemist to tune the metal loading, optimise the surface distribution of active sites and their availability as well as select the most suitable oxidic support in terms of specific surface area, porosity, morphology and hydrophobic/hydrophilic character.

In the field of heterogeneous oxidation catalysts, a very broad series of effective catalysts have been prepared anchoring metallic precursors onto previously structured silica supports. Inorganic salts or organometallic precursors of titanium, vanadium, tantalum, zirconium or niobium proved to be the most suitable starting compounds and the active sites were mainly generated on mesoporous silica molecular sieves [3,4,5,6,7]. Titanium-grafted silica catalysts are the first of this class of solids and have been successfully applied to the selective transformation of alkenes into epoxides, (cyclo)alkanes into alcohols or ketones, sulphides into sulphoxides, thiophenes into sulphones, alcohols into aldehydes or ketones, arenes into phenols, phenols into benzoquinones, etc. [8,9]. Titanium-grafted silicate catalysts have shown promising performance, especially in the presence of bulky and richly-functionalised substrates. Nevertheless, the optimal performance of titanosilicalite-1 zeotype, TS-1, in selective oxidation is still unparalleled, in terms of selectivity, activity and robustness of the catalyst structure [10]. Then, some attention was attracted by vanadium, tantalum and zirconium-grafted species, which, on the contrary, showed scarce stability to leaching in liquid-phase reaction media (especially for vanadium-based systems) or limited results in terms of activity [11,12,13,14,15]. More recently, niobium-silicate catalysts displayed interesting catalytic performance, in water-containing reaction media too, thanks to their enhanced

robustness against hydrolysis due to the more optimal geometry of Nb-O-Si bond angles compared to V-O-Si [16]. The number of studies showing the successful application of Nb-containing systems in the presence of hydrogen peroxide as an oxidant has therefore rapidly increasing accordingly, in the last years [17,18,19]. Grafted catalysts based on Group 6 organometallic precursors, on the other hand, have been somehow neglected in this restless quest for the optimal metal-grafted silica catalyst for selective oxidations. This is undoubtedly due to the scarce resistance to leaching of chromium- and molybdenum-containing systems and their intrinsic higher activity when the metal sites are dissolved in homogeneous phase, rather than deposited on the oxidic support [20,21]. In some cases, these catalysts did not show a genuine heterogeneous nature, especially in the presence of aqueous hydrogen peroxide or when water-containing reaction media were used [22]. With regard to tungsten, very good results have been recorded, in the last decades, in the epoxidation of alkenes under homogeneous and/or biphasic conditions [23,24,25,26], although these systems often show, as a major drawback, a difficult separation and recovery of the spent catalyst. However, some recent works have paid attention to tungsten-based heterogeneous catalysts for the selective oxidation of alkenes with hydrogen peroxide too [25,27,28,29,30,31,32,33,34,35]. Tungsten-silica catalysts prepared by simple impregnation of the metal precursor onto porous siliceous molecular sieves typically led to uneven surface  $WO_3$  domains, which are thus prone to further aggregation, activity loss and scarce robustness [36,37]. For this reason, the most suitable strategy appeared to obtain isolated W species grafted onto silica through W-O-Si covalent bonds [38]. Some of them displayed promising performances in terms of activity and/or selectivity to desired epoxides. Other systems, on the contrary, showed modest results either in terms of specific activity with values in the range of  $10 \text{ h}^{-1}$  (moles of converted alkene per mole of W per hour) [39] or because of a remarkable loss of active metal in the reaction medium [40,41,42,43,44,45]. In some successful cases, it was shown that, even though a non-negligible leaching of tungsten was observed from the solid into the reaction mixture, such W species were not able to act as homogeneous catalysts by themselves, hence confirming the heterogeneous behaviour of the studied tungsten catalyst [32].

In this aim, in the present work, we describe a detailed spectroscopic study about the nature of tungsten species deposited onto the mesoporous silica following two post-synthesis approaches: a liquid-phase grafting and an alternative, less environmentally unfriendly, solventless synthesis protocol based on dry impregnation, DI, of *bis*(cyclopentadienyl)tungsten(IV) dichloride,  $W(Cp)_2Cl_2$ . Finally, the catalytic features of the obtained sites were studied and compared in the liquid-phase epoxidation of two model alkene substrates: an unsaturated terpene, limonene, and an unsaturated fatty acid methyl ester, methyl oleate.

## EXPERIMENTAL DETAILS

### Catalyst Preparation

Tungsten-silica catalysts were all prepared by grafting *bis*(cyclopentadienyl)tungsten(IV) dichloride ( $W(Cp)_2Cl_2$ ; 99% Strem Chemicals) onto a commercially available amorphous pure silica support (Grace Davison, Davisil SiO<sub>2</sub> LC60A, 60-200  $\mu$ m). The silica support was pre-treated under dry air at 500°C for 1 h, then left at 500°C for 1 h in vacuo and finally cooled to room temperature in vacuo as well, in order to remove any potential organic contaminant on the surface.

The W/SiO<sub>2</sub>-DI catalyst, obtained via dry impregnation, was prepared by adapting a method previously adopted for Ti(Cp)<sub>2</sub>Cl<sub>2</sub> and Nb(Cp)<sub>2</sub>Cl<sub>2</sub> [18]. The silica support was hydrated with high-purity deionized water (MilliQ Academic, Merck Millipore, 18 M $\Omega$ -cm) for 2 h, dried at the rotary evaporator and then pre-treated in air at 300°C for 1 h and in vacuo overnight at 300°C.  $W(Cp)_2Cl_2$  was finely ground and mixed to the silica support, under inert atmosphere. The solid mixture was continuously stirred overnight under steady vacuum at room temperature (20°C; in thermostatic bath). The resulting light brown powder was calcined under dry oxygen at 500°C for 2 h in order to obtain the final W(VI)-silica catalysts.

The W/SiO<sub>2</sub>-liq catalyst, prepared via liquid-phase grafting, was obtained modifying the method previously described for titanium and niobium [46,47] and adapting it to *bis*(cyclopentadienyl)tungsten(IV) dichloride. In this case,  $W(Cp)_2Cl_2$  was dissolved in anhydrous CHCl<sub>3</sub> (Prolabo, RP; dried over 3A molecular sieves) under argon. The resulting solution was added to the pre-treated silica and stirred for 60 min at room temperature. Freshly distilled triethylamine

was then added to the suspension and left under stirring overnight. The solid was filtered on a Büchner funnel, washed with fresh  $\text{CHCl}_3$  and dried for 3 h. It was calcined at  $550^\circ\text{C}$  under dry oxygen ( $80 \text{ mL min}^{-1}$ ) for 6 h.

Pure commercial  $\text{WO}_3$  (Sigma-Aldrich, puriss. 99.9%) was used for comparison with no further modifications.

### **Catalyst Characterization**

The tungsten content of the prepared samples was determined by inductively coupled plasma optical emission spectroscopy (ICAP 6300 Duo, Thermo Fisher Scientific) after mineralization of the samples in a microwave digestion apparatus (Milestone MLS 1200; maximum power 500 W) with a mixture of hydrofluoric acid (aq. 40%) and fuming nitric acid.

Diffuse reflectance UV–Visible spectra were collected using a Perkin Elmer Lambda 900 spectrometer equipped with an integrating sphere accessory and using a hand-made quartz cell allowing analysis both under vacuum conditions (residual pressure  $10^{-5}$  mbar) and under controlled gas atmosphere. Prior the analysis, the samples were dispersed in anhydrous  $\text{BaSO}_4$  (10 wt.%).

Raman spectra were recorded in the  $4000\text{--}50 \text{ cm}^{-1}$  range, using a resolution of  $4 \text{ cm}^{-1}$  with 2000 scans, using a RFS 100 Bruker FT-Raman spectrometer equipped with a 1064 nm wavelength excitation laser. Laser power was set at 100 mW. Raman spectra were elaborated by using OPUS 5.0 software (Bruker Optics Company).

X-ray diffractograms (XRD) were collected on unoriented ground powders with a Thermo ARL ‘XTRA-048 diffractometer with a  $\text{Cu K}\alpha$  ( $k = 1.54 \text{ \AA}$ ) radiation. Diffractograms were recorded at room temperature with a step size of  $0.02^\circ$  and a rate of  $1^\circ 2\theta \text{ min}^{-1}$ .

$\text{N}_2$  physisorption measurements were carried out at 77 K in the relative pressure range from  $1 \times 10^{-6}$  to  $1 \text{ P/P}_0$  by using a Quantachrome Autosorb 1MP/TCD instrument. Prior to analysis, the samples were outgassed at 373 K for 3 h (residual pressure lower than  $10^{-6}$  mbar). Apparent surface areas were determined by using Brunauer–Emmett–Teller equation, in the relative pressure range from 0.01 to

0.1 P/P<sub>0</sub>. Pore size distributions were obtained by applying the NLDFT method (N<sub>2</sub> silica kernel based on a cylindrical pore model applied to the desorption branch).

#### *X-ray Absorption Spectroscopy*

The XAS data for the W L<sub>3</sub> and L<sub>1</sub> edges were collected at room temperature and under air at the beamline 4-1 and 4-3 at the Stanford Synchrotron Radiation Lightsource (SSRL) operating with an energy of 3 GeV and a current of 500 mA. The samples were packed inside the sample holder under ambient atmosphere and the fluorescence data were collected by a Lytle detector. In order to improve the signal to noise ratio each run has been repeated at least four times.

The collected data were analyzed with Athena and Artemis software programmes [48] in order to obtain the coordination number (N), the distance of the scattering atoms (R) and the disorder  $\sigma_{DW}$  factor of the neighbour scattering atoms (v. Table S1; Supplementary Material).

#### **Catalytic tests**

The epoxidation reaction tests on (*R*)-(+)-limonene (97%, Sigma) and methyl oleate (99% Aldrich) were carried out in a round-bottomed glass batch reactor, in an oil bath set at 90°C, with magnetic stirring (*ca.* 800 rpm) under dry nitrogen atmosphere. The W/SiO<sub>2</sub> catalysts were pre-treated in dry air at 500°C and cooled down to room temperature in vacuo prior to use. WO<sub>3</sub> was pre-treated either at 120°C in dry air for 1 h and then in vacuo for 1 h or at 500°C in dry air and cooled down to room temperature in vacuo prior to use.

The catalyst (100 mg) was dispersed in 5 mL of acetonitrile (Aldrich, HPLC grade), as solvent, in the presence of 1 mmol of substrate (either limonene or methyl oleate) and 2 or 4 mmol of aqueous hydrogen peroxide (H<sub>2</sub>O<sub>2</sub>; 50% Aldrich), as oxidant (oxidant to substrate molar ratio of 2 : 1 or 4 : 1). *Tert*-butylhydroperoxide, TBHP (Sigma-Aldrich; 5.5 M anhydrous solution in decane) was used in one test with an oxidant to substrate molar ratio of 1.1 : 1. Samples were withdrawn from the reaction medium at regular intervals and analysed by GC (Agilent 6890 Series; SP-5 column, 30 m × 0.25 mm; FID detector), by using mesitylene (puriss. ≥ 99%, Fluka,) or methyl palmitate (≥ 99%, Sigma) as internal standards, for limonene or methyl oleate epoxidation, respectively. Gas-chromatographic peaks were identified by comparison with peaks of genuine samples of standard compounds and confirmed by means of GC-MS. For both limonene epoxide and methyl

epoxystearate, *cis:trans* ratios were determined by  $^1\text{H-NMR}$  analysis (Bruker DRX 300) of the 6 h reaction mixture, after solvent removal in vacuo. A standard deviation of  $\pm 2\%$ ,  $\pm 4\%$  and  $\pm 2\text{ h}^{-1}$  has to be considered on average for the conversion, yield and specific activity values, respectively. All tests were replicated at least two times. No significant oxidation reactivity was recorded in the absence of solid catalyst or in the presence of the pure silica support (in the absence of tungsten loading). A maximum limonene conversion of *ca.* 5–6% was observed after 6 h of reaction, but with no noteworthy formation of epoxide products. Analogously, a maximum methyl oleate conversion of *ca.* 7% was recorded after 6 h, with very minor traces of the related epoxide, methyl epoxystearate. After each test, the presence of residual hydrogen peroxide was checked and confirmed by iodometric assays.

In order to check the possible leaching of tungsten species, the solid catalyst was removed from the liquid mixture after 45 min by hot centrifugation (at the same temperature of the reaction mixture) and the filtered liquid solution was tested for further reaction [49]. In the tests for the recovery of the catalyst, the solid was separated by filtration and thoroughly washed with acetonitrile and then with methanol (Fluka, HPLC grade). The filtered solid was dried gently at  $110^\circ\text{C}$ , weighed, activated again at  $500^\circ\text{C}$  under dry air and then reused in a new catalytic cycle as described above. In one limonene epoxidation test, hydroquinone (Carlo Erba; p.a.) was used as a free-radical scavenger in a quasi-equimolar amount (0.8 : 1 mol/mol) with respect to the total tungsten content in the catalyst and added to the reaction mixture under the same conditions reported above.

## RESULTS AND DISCUSSION

### Catalyst preparation

In the present work, at the best of our knowledge, two tungsten-containing silica catalysts were prepared for the first time via deposition of tungstenocene(IV) dichloride over a cheap and commercially available non-ordered mesoporous silica support. The selected commercial silica displays a relatively high specific surface area ( $605\text{ m}^2\text{ g}^{-1}$ ; Table 1), thus providing a sufficient surface for the deposition of the organometallic precursor. Then, the silica support was first calcined at  $500^\circ\text{C}$  in order to remove from the surface undesired organic impurities that might contaminate the

solid. However, such treatment can lead to an extended condensation of the surface silanol groups and a reduction of the grafting points for the metallocene precursor. So, the support was first re-hydrated with pure water and then treated at lower temperature, 300°C [50].

At the end the dry impregnation process, the freshly prepared W/SiO<sub>2</sub>-DI sample (before final calcination) showed a uniform greenish-brownish colour, suggesting an even deposition of the metal species. Then, by means of the calcination under oxygen, the organic cyclopentadienyl ligands were oxidised and removed. In that step, the catalytically active W(VI) centres were also obtained on the silica surface. The amount of tungstenocene precursor added into the dry-impregnation mixture was chosen to obtain a metal loading of *ca.* 2 wt.%, since 1 to 2 wt.% was observed to be, in general, an optimal Ti, Nb or W loading for the epoxidation of a large variety of alkenes [51,32]. In addition, a metal loading of 2 wt.% on this kind of silica (with a specific surface area of 605 m<sup>2</sup> g<sup>-1</sup>; Table 1) approximately corresponds to 0.10 tungsten atoms per square nanometer. This surface tungsten density is sufficiently lower than the value of *ca.* 0.3 W atoms nm<sup>-2</sup>, which is widely accepted as a good approach to have an adequate metal loading and a homogeneous dispersion of the metal sites on the porous silica support [52,53]. Beyond that limit undesirable large aggregates of WO<sub>x</sub> species may occur on the catalyst surface. Nevertheless, the actual metal content showed that only a part of the expected metal was present (Table 1). A part of the tungsten precursor was lost, likely deposited on the walls of the glass vessels where the dry impregnation process took place and/or aspired by the vacuum pump during the evacuation procedure. Anyway, the elemental analysis of different aliquots of catalyst powder, sampled randomly on the same batch, confirmed the even dispersion of the W species on silica support.

At the same time, one W/SiO<sub>2</sub>-liq catalyst was prepared via metallocene grafting in liquid phase and used as a comparison with respect to the solid obtained via dry impregnation. It is worth highlighting, however, that the dry impregnation route is conceptually simpler and does not require the use of a hazardous and environmentally unfriendly solvent or of a base (*i.e.*, chloroform and triethylamine, respectively). Anyway, the scarce solubility of W(Cp)<sub>2</sub>Cl<sub>2</sub> in chloroform led to a limited deposition

of the organometallic precursor and an amount lower than expected of tungsten was therefore grafted onto the final solid (1.2 wt.% vs. expected 2 wt.%).

### Physico-chemical characterization of W-containing silica catalysts

The grafting of *bis*(cyclopentadienyl)tungsten(IV) dichloride precursor in both W/SiO<sub>2</sub>-liq and W/SiO<sub>2</sub>-DI samples was monitored by diffuse reflectance UV-Visible spectroscopy (Fig. 1). The DR UV-Visible spectra of the two samples before calcination clearly show a band at 230 nm assigned to W–O charge-transfer transitions and other two absorptions around 270 nm and *ca.* 400 nm ascribed to the transitions of the residual cyclopentadienyl groups attached to the metal site, in agreement with literature data reported for similar catalysts [41,54]. Similar absorptions at 270 nm and in the 330–470 nm range were observed in the spectrum of the pure *bis*(cyclopentadienyl)tungsten(IV) dichloride precursor (Fig. S1; Supplementary Material). However, the wide broadening of these bands in the spectrum of *bis*(cyclopentadienyl)tungsten(IV) dichloride may be tentatively ascribed to hydrophobic molecular aggregation. The amount of tungsten deposited onto the silica surface in the two samples was measured after calcination of the organic fraction, and was 1.18 for W/SiO<sub>2</sub>-liq and 1.70 for W/SiO<sub>2</sub>-DI sample, respectively (Table 1).

The textural properties of the two catalysts were investigated by N<sub>2</sub> physisorption analysis at 77 K and the specific surface area (SSA) and pores volume and diameter were determined by Brunauer–Emmett–Teller method and NLDFIT approach. Both samples (prepared by liquid-phase grafting and dry impregnation) showed N<sub>2</sub> physisorption isotherms of type IV with H2 hysteresis loop. These isotherms are typically observed for porous materials characterized by an irregular pore size (Fig. 2).

The specific surface area of the W/SiO<sub>2</sub>-liq sample is *ca.* 603 m<sup>2</sup>g<sup>-1</sup> and is comparable to the one of the pristine siliceous support. This behaviour is in line with previous observations on niobium-containing catalysts [18]. Such a result is a clear indication that the liquid grafting did not modify the textural features of the starting material. Moreover, W/SiO<sub>2</sub>-liq catalyst displays a disordered pore size distribution in the 2–10 nm range, with a relative pore volume of 1.38 cm<sup>3</sup> g<sup>-1</sup>. Such unusual increase of the specific pore volume with respect to the pristine SiO<sub>2</sub> is probably due to a different

aggregation of the secondary larger silica particles/grains during the various liquid-phase grafting treatments (dispersion in solvents, calcination, etc.). For these non-ordered mesoporous materials, the porosity is partially linked to particles aggregation, that can be affected by the synthetic procedure adopted for the catalyst preparation. A completely different scenario was observed for W/SiO<sub>2</sub>-DI sample. In this case, a marked reduction of specific surface area to 465 m<sup>2</sup> g<sup>-1</sup> was observed after the impregnation process (Table 1). The differences in the textural properties of the two catalysts may be associated to a different organization and distribution of the tungsten sites in the solids promoted by the two synthetic procedures.

The coordination and chemical environment of the W(VI) sites obtained after calcination and distributed on the silica surface were studied by DR UV-Vis spectroscopy (Fig. 3). The spectra of both samples show two important bands at *ca.* 250 and 320 nm ascribed to metal-ligand charge transfer in partially isolated sites or organized in tungsten oxides with nanometric dimensions with different coordination geometry (tetrahedral and octahedral), formed during the deposition of tungsten [55]. Further information about the nature and the coordination chemistry of these metal sites can be obtained through XAS experiments (*see below*).

Moreover, the DR UV-Visible spectrum of W/SiO<sub>2</sub>-DI catalyst (Fig. 3b) shows an additional wide band centred at *ca.* 380 nm, not detectable on the sample prepared via liquid-phase grafting process. This band is tentatively attributed to the formation of large tungsten oxide domains dispersed on the surface. The presence of these metal oxide domains was also confirmed by other spectroscopic (Raman) and structural analyses (X-ray diffraction).

Transition metal oxides, as they are typically characterized by a high structural symmetry, are suitable to be characterized by Raman spectroscopy. The Raman spectrum of commercial monoclinic WO<sub>3</sub> sample exhibits some sharp peaks at 805, 715, 325 and 270 cm<sup>-1</sup>, assigned to octahedral tungsten oxide units (Fig. 4) [55]. The first two peaks at high wavenumbers were also detected in the Raman spectrum of W/SiO<sub>2</sub>-DI sample. The presence of these two peaks reveals the formation of octahedral microdomains of tungsten oxide promoted by the calcination process (Fig. 4), in agreement with DR

UV-visible data. Interestingly, these two peaks were completely absent in the spectrum of W/SiO<sub>2</sub>-liq sample, in which the metal centres were isolated and distributed more homogeneously than in the sample prepared via dry impregnation (Fig. 4).

The crystallographic phase of the tungsten oxide domains in the sample prepared via dry impregnation was studied by X-ray diffraction technique too. The X-ray profiles of W/SiO<sub>2</sub>-liq and W/SiO<sub>2</sub>-DI samples are reported in Figure 5, where they are compared with the XRD pattern of the commercial WO<sub>3</sub> sample. The diffractogram of the sample prepared by liquid grafting is characterized by a broad band at 22° 2 $\theta$ , typical of amorphous silica (Fig. 5, curve a). Furthermore, no signals typical of large tungsten oxide aggregates were present. These results are in agreement with the DR UV-Visible spectroscopy data and they suggest that the W(VI) sites of W/SiO<sub>2</sub>-liq were well-distributed on the silica surface. In contrast, the diffractogram of the sample prepared by dry impregnation (Fig. 5b) shows, along with the wide band centred at 22° 2 $\theta$ , some weak reflections at 23.2°, 23.6°, 24.2° 2 $\theta$ , which are attributed to the presence of larger tungsten oxide aggregates. By a direct comparison with the X-ray profile of the commercial monoclinic WO<sub>3</sub> sample, the microdomains of oxide distributed on the silica surface for the W/SiO<sub>2</sub>-DI sample can be attributed to a monoclinic structure. The set of data explained above indicates that the dry impregnation process, although leading to a material with higher tungsten metal content, was also associated to the formation of oxidic domains dispersed over the silica surface.

### **X-ray Absorption Spectroscopy characterization**

The normalized XANES data for L<sub>1</sub> and L<sub>3</sub> edges are reported in Figure 6, 7, S2 and in table S1 (Supplementary Material). While the main edge features for the L<sub>1</sub>-edge were similar for all the samples (Fig. 6a), confirming the presence of W(VI) on the silica support, differences were clear in the pre-edge region (Fig. 6b). The pre-edge feature at *ca.* 12100 eV in the W L<sub>1</sub>-edge is due to the 2*s*-5*d* dipole-forbidden transition for a pure octahedral geometry and its intensity increases with the degree of distortion around the W sites from pure octahedral to tetrahedral geometry, due to the loss of the centre of inversion of symmetry and progressive mixing of empty *p-d* states [56]. The strong

pre-edge peak for the sample synthesized from liquid (Fig. 6b) is therefore related to a higher distortion of the  $\text{WO}_6$  unit compared to  $\text{W/SiO}_2\text{-DI}$ , being the intensity of pre-edge peak of the latter closer to  $\text{WO}_3$ . The pre-edge intensity for  $\text{W/SiO}_2\text{-liq}$  is however weaker than expected for well-isolated  $\text{WO}_4$  unit [57], supporting the presence of mainly  $\text{WO}_6$  sites in all samples.

The position of the white line for the  $\text{L}_3$ -edge of the two samples (Fig. 7a) was comparable to the one of the  $\text{WO}_3$  standard, in agreement with the presence of  $\text{W(VI)}$ . However, differences in the shape were clearly visible, especially in the second derivative plot (Fig. 7b). The  $\text{W L}_3$ -edge is mainly due to the dipole-allowed transition from the metal  $2p_{3/2}$  orbitals to vacant  $d$  orbitals and its splitting is related to the geometry of the  $\text{W}$  site. In fact, a larger splitting is expected for an octahedral site and a smaller one for a tetrahedral one, as a result of the different energy splitting of the  $d$  orbitals due to the different ligand field [58]. A splitting of 3.0 -4.0 eV is generally indicative for distorted  $\text{WO}_6$ , while a splitting of 1.8-2.0 eV is typical for  $\text{WO}_4$  moieties [59]. The second derivative of the white line, reported in Figure 7b, clearly shows two distinct minima for  $\text{WO}_3$  and the  $\text{W/SiO}_2$  samples. The energy separation of 3.1 eV and 3.9 eV for  $\text{W/SiO}_2\text{-liq}$  and for  $\text{W/SiO}_2\text{-DI}$ , respectively, prove the presence of distorted octahedral  $\text{WO}_6$  units in both solids. The smaller value for the sample synthesized via liquid-phase grafting is consistent with a higher distortion of the  $\text{W}$  sites as well (*vide supra*  $\text{L}_1$ -edge).

The strong peaks between 1 Å and 2 Å shown in the FT of the EXAFS oscillation for the two samples are the results of different  $\text{W-O}$  scattering paths in the  $\text{WO}_6$  unit (Fig. 8). While  $\text{W/SiO}_2\text{-DI}$  presented only one broad peak, similar to  $\text{WO}_3$ ,  $\text{W/SiO}_2\text{-liq}$  showed a splitting of the first shell into two different peaks at shorter and a longer distance, reflecting the higher distortion of the  $\text{WO}_6$  unit [60]. The quantitative results of the fitting reveal three different  $\text{W-O}$  bonds for  $\text{W/SiO}_2\text{-liq}$  (Table SII): two short bonds at 1.72 Å and 1.91 Å and a longer one at 2.26 Å. This long  $\text{W-O}$  bond is consistent with the high distortion of the octahedral unit and is characteristic of hydrated tungsten oxide polyoxo clusters species [61]. The results for  $\text{W/SiO}_2\text{-DI}$  are instead comparable to  $\text{WO}_3$  ( $\text{W/SiO}_2\text{-DI}$ : 1.75 Å and 2.04 Å;  $\text{WO}_3$ : 1.81 Å and 2.11Å) and in agreement with the presence of  $\text{WO}_3$  domains for this

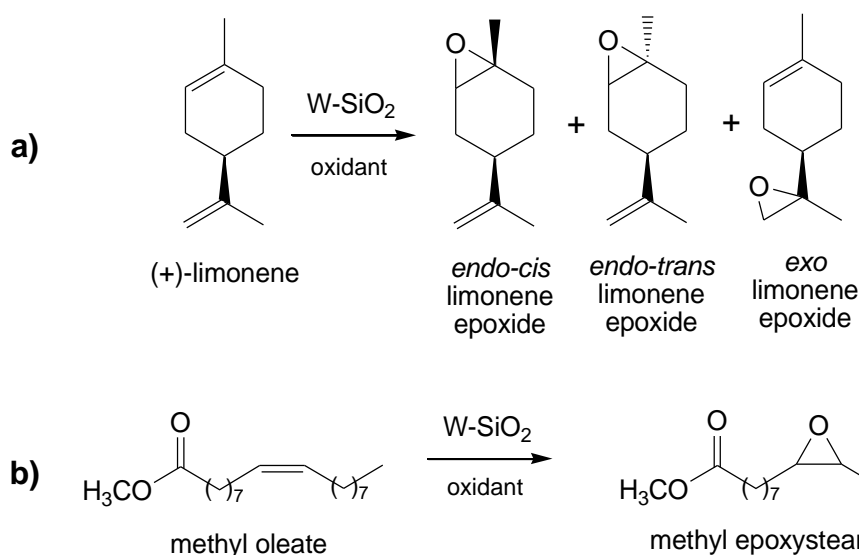
sample. A second peak between 2.3 Å and 3.2 Å and a third one centred at 3.5 Å (non-phase shift corrected distances) were present in the EXAFS of both WO<sub>3</sub> and W/SiO<sub>2</sub>-DI, confirming the similar nature of the W site for the two samples. The first peak derives from multiple scattering within the first shell (W-O-O) while the second one is related to W-W scattering path for corner-shared WO<sub>6</sub>. Notably, the shorter distance of the W-W shell for W/SiO<sub>2</sub>-liq evidences the presence of edge-shared WO<sub>6</sub> typical of octahedrally coordinated small oligomeric tungsten oxide species confirming the quantitative EXAFS analysis of the W-O shell and the XANES analysis of L<sub>1</sub> and L<sub>3</sub> edges [62]. The peak at 2.7 Å (non-phase shift corrected distance) for this sample may be assigned to W-Si scattering path [63].

Interestingly, previous studies have already revealed the presence of both WO<sub>3</sub> domains and hydrated tungsten oxide polyoxo clusters under ambient conditions on the silica surface. Upon dehydration, only the latter species decompose to isolated surface monoxo- and dioxo-isolated W species [64,65,66].

The combination of UV-visible and X-ray absorption spectroscopy studies revealed that the coordination geometry and structure of tungsten sites are markedly different in the two catalysts and are strongly dependent on the adopted synthetic procedure. Tentatively, we can conclude that well-dispersed tungsten oxide polyoxo cluster sites are mainly distributed on the surface of sample prepared via liquid-phase grafting, whereas monoclinic domains of tungsten oxide are clearly detected on the surface of W/SiO<sub>2</sub> sample.

### **Catalytic tests**

The tungsten-grafted silica catalysts described above have been evaluated in the selective liquid-phase epoxidation of two alkenes: limonene and methyl oleate.



Scheme 1

By studying the epoxidation of limonene, it is possible to evaluate not only the activity and chemoselectivity of the catalysts, but also their regio- and stereoselectivity (Scheme 1a). The performance of the two catalysts, namely  $W/SiO_2$ -liq and  $W/SiO_2$ -DI, were compared to the one of a commercial batch of  $WO_3$  (Table 2).

All of the W-containing systems were active in the epoxidation of limonene, when aqueous hydrogen peroxide was used as an oxidant, and moderate to good values were achieved, in terms of alkene conversion (up to 80%, after 6 h) and yield to epoxides (up to 54%, after 6 h). Clearly, specific activity values for  $WO_3$  catalysts were very low, because of the very high (nominal) tungsten content in the bulk of pure tungsten oxide samples.  $W/SiO_2$ -DI showed the best performance in terms of specific activity per W site, confirming that the non-negligible presence of aggregated oxidic domains (as revealed by DR UV-Vis and XAS studies; *see above*) is not a detrimental feature for the epoxidation reaction.

Limonene epoxides were produced with good selectivities (in the range 60 to 68%) and the formation of the oxirane ring on the 1,2- and 8,9-C=C double bonds was predominant with respect to the formation of carveols, which are conversely obtained via allylic oxidation of the endocyclic unsaturation, via a radical oxidation pathway. Carveols and other allylic cyclic terpenic alcohols were indeed the major side products. However, non-negligible amounts of menthenediols, derived from the water-mediated opening of the oxirane rings, were observed as well. This behaviour suggests that over W-silica systems the concurrent formation of oxidized products via homolytic oxidation of limonene by  $H_2O_2$ -derived radicals played a less

relevant role than the heterolytic oxygen transfer from  $\text{H}_2\text{O}_2$  to the alkene group. Conversely, when anhydrous *tert*-butylhydroperoxide, TBHP, an oxidant that is particularly suitable for use under water-free conditions on Ti-based systems [11,67], was used, limonene indeed underwent oxidation, but no selective production of epoxides was detected. In this case, a very large number of minor side-products, generated by radical species derived from TBHP decomposition, was observed. In terms of regioselectivity, the molar ratio between endocyclic to exocyclic limonene epoxides (Scheme 1a) was *ca.* 80:20 over all the catalysts. This result is fully consistent with the values previously observed over other Ti-silica systems and suggests that the oxygen transfer preferentially takes place on the electron-rich endocyclic unsaturation [47,68,69]. Finally, a similar *cis* to *trans* limonene epoxide molar ratio (*ca.* 80:20) was recorded for all of the W-containing catalysts. Such preferential trend towards the *cis* epoxide suggests that over both grafted and bulk  $\text{WO}_3$  systems the oxygen-transfer primarily occurs on the less hindered face of the cyclohexene ring, both methyl and *iso*-propenyl groups (on C1 and C4 carbons, respectively) pointing towards the opposite face of the epoxy ring (Scheme 1a). In one test, hydroquinone was used a radical scavenger in a quasi-equimolar amount with respect to the total tungsten species in the W-SiO<sub>2</sub> catalyst. A modest slowdown of the epoxidation activity was observed (specific activity after 1 h decreased to 24 h<sup>-1</sup> and 21 h<sup>-1</sup>, for W/SiO<sub>2</sub>-liq and W/SiO<sub>2</sub>-DI, respectively), but the reactivity was not suppressed. These experimental observations suggest that the role of a radical-mediated pathway is small, although non-negligible, over these catalysts, under these conditions.

Since metal leaching is the main drawback W-silica catalysts suffer from, especially in the presence of aqueous hydrogen peroxide [32,40,41,43], the actual heterogeneous nature of W/SiO<sub>2</sub>-DI was examined in a hot-centrifugation test and compared to the results obtained over commercial  $\text{WO}_3$  (Figure 9). Under the tested conditions, the production of limonene epoxides did not stop when  $\text{WO}_3$  was centrifuged out from reaction mixture, after 45 min, whereas W/SiO<sub>2</sub>-DI showed a genuinely heterogeneous nature, with no further conversion of limonene into the related epoxide after the solid was removed from the liquid phase. From a visual point of view too, the reaction mixtures containing the  $\text{WO}_3$  sample rapidly turned into a greenish-brownish colour (in few minutes), after the addition of the aqueous  $\text{H}_2\text{O}_2$ . On the contrary, no evident changes in colour were observed in the presence of the W/SiO<sub>2</sub>-DI solid. This behaviour confirms that no active soluble species leached out from W/SiO<sub>2</sub>-DI, whereas most of the catalytic activity of the

commercial  $\text{WO}_3$  sample has to attributed to homogeneous tungsten species present and active in the liquid phase.

The  $\text{W}/\text{SiO}_2\text{-DI}$  sample was then studied in a series of repeated catalytic cycles, up to six runs (Figure 10). It is worth highlighting that an intermediate calcination step (in dry air at  $500^\circ\text{C}$ ) was always necessary in order to recover most of the pristine catalytic activity. The thermal regeneration step is indeed necessary to get rid of the organic heavy deposit that might have fouled the active centres, thus hindering a proper recovery of the catalytic activity [32]. Nevertheless, even after such regeneration step, a gradual loss in catalytic performance was recorded along the six recycling runs, with a more remarkable diminution between the first and the second run as well as between the fifth and sixth one. On the contrary, no remarkable changes in epoxide selectivity were observed.

The amount of soluble W species in the liquid mixture after the hot centrifugation tests was quantified for both solids by ICP-AES analysis. After the first recycle, that is usually the most prone to metal leaching, values of 9 and 60 ppm of tungsten metal were found in the liquids that contained  $\text{W}/\text{SiO}_2\text{-liq}$  and  $\text{W}/\text{SiO}_2\text{-DI}$ , respectively. The release of metal species into solution from the sample obtained via dry impregnation method was thus higher than the one prepared via liquid-phase grafting. Such leaching values are, on average, lower than those reported in the previous literature, especially when polar protic solvents were used as reaction media (37,40,70). This behaviour does not show a massive leaching of metal species into the reaction mixture. From the spectroscopic point of view, the distribution of the isolated and organized nanosized tungsten oxide domains appeared slightly different after six catalytic cycles. The UV-Visible band at *ca.* 300-320 nm, assigned to the presence of small domains of  $\text{WO}_3$  species, was more evident in the recycled catalyst (Fig. S3; Supplementary Material). Therefore, the gradual loss in the catalytic performance of  $\text{W}/\text{SiO}_2\text{-DI}$  is likely to be attributed to the alteration of the tungsten species located on the silica surface rather than to a massive leaching of catalytically active metal.

$\text{W}/\text{SiO}_2\text{-liq}$  and  $\text{W}/\text{SiO}_2\text{-DI}$  were, in addition, studied in the epoxidation of methyl oleate, as a widely accepted model substrate for unsaturated oleochemicals [71,72] (Scheme 1b). With the noteworthy exception of

heterogenised polyoxotungstate species [73,74], to our best knowledge, no tungsten-containing heterogeneous silica catalysts have been used for the epoxidation of unsaturated oleochemicals so far.

The performance of the two catalysts were modest, in terms of yield (towards the desired methyl epoxystearate) and specific activity, in comparison with other systems previously described in the literature [75,76]. After 6 h of reaction, a maximum epoxide yield of *ca.* 50% was reached, the average values being around 30% (Table 3). Under these conditions, allylic oxidation products, such as methyl hydroxyoleate, were scarcely observed, the major side products being methyl dihydroxystearate derived from water-mediated opening of the oxirane ring.

Thanks to a higher oxidant-to-alkene ratio (4:1 vs. 2:1 mol/mol), higher conversion and yield values were achieved on both catalysts. Actually, when a 2:1 ratio only was used, hydrogen peroxide was entirely consumed and no residual unreacted H<sub>2</sub>O<sub>2</sub> was detected by iodometric assay at the end of 6h of reaction. The oxidant efficiency (the amount of oxidised products obtained per amount of consumed H<sub>2</sub>O<sub>2</sub>) was, on average, quite scarce over these catalysts. Values always lower than 50% were indeed recorded due to the unproductive decomposition of hydrogen peroxide into water and molecular oxygen. A larger excess of H<sub>2</sub>O<sub>2</sub> (4:1 molar ratio) was thus necessary to push further the epoxidation reaction. In terms of specific activity, the best performance was obtained over W/SiO<sub>2</sub>-liq with a four-fold excess of oxidant, whereas, if one considers the yield towards the desired epoxide only, the best result was achieved over W/SiO<sub>2</sub>-DI, as it was the case for the limonene epoxidation too.

Interestingly, by monitoring through <sup>1</sup>H-NMR spectroscopy the *cis-to-trans* ratio in the formed methyl epoxystearate at the end of the reaction, a noteworthy amount of the *trans* isomer was found (from 15% to 42% of the overall epoxide). Since the configuration of the parent methyl oleate is *cis* only, these values are a clear clue that a radical-driven oxidation of the C=C bond occurred, with a consequent partial recombination of the geometry around carbon-9 and carbon-10. In fact, if a free-radical epoxidation pathway prevails over a heterolytic one, the formation of the *trans* isomer, the thermodynamically more stable form, is predominant [77,78,79].

## CONCLUSIONS

Tungstenocene(IV) dichloride proved to be a suitable precursor for the preparation of W(VI)-grafted silica catalysts to be used in the epoxidation of alkenes. The catalyst preparation via a dry impregnation grafting approach was simple, versatile and did not require the use of hazardous or environmentally unfriendly solvents. The spectroscopic characterization of W/SiO<sub>2</sub>-liq and W/SiO<sub>2</sub>-DI samples evidenced that W(VI) sites were fairly evenly distributed on the silica surface for both systems. However, the W/SiO<sub>2</sub>-DI catalyst displayed the presence of larger monoclinic tungsten(VI) oxide aggregates, whereas the W/SiO<sub>2</sub>-liq sample showed mainly well-dispersed tungsten oxide polyoxo cluster sites. Indeed, the chemical environment and the coordination geometry of W(VI) sites were noticeably different in the two systems and were strongly dependent on the synthetic protocol adopted for their preparation.

When these catalysts were tested in the epoxidation of (+)-limonene and methyl oleate, as model alkene substrates, both catalysts were active in the presence of aqueous hydrogen peroxide and W/SiO<sub>2</sub>-DI showed the best performance, on average, in terms of yield to desired epoxides. The genuine heterogeneous nature of the grafted W/SiO<sub>2</sub>-DI catalyst was successfully confirmed by a hot-centrifugation heterogeneity test and the solid could be reused and recycled up to five times with a gradual loss in activity, before showing a clear diminution in the performance at the sixth one. On the contrary, under the same reaction conditions, a reference commercial WO<sub>3</sub> sample showed, at the first run, a remarkable leaching of homogeneously active tungsten species into the reaction mixture.

The W/SiO<sub>2</sub>-DI system was therefore a good compromise between an adequate interaction of the tungsten sites with the silica surface, thus providing the catalyst with an satisfactory robustness against leaching, and an even dispersion of the tungsten oxide domains over the support, thus providing the catalyst with a good catalytic activity per metal site.

## ACKNOWLEDGMENTS

Use of the Stanford Synchrotron Radiation Lightsource, SLAC National Accelerator Laboratory, is supported by the U.S. Department of Energy, Office of Science, Office of Basic Energy Sciences under Contract No. DE-AC02-76SF00515.

## REFERENCES

## References

- [1] M. K. Samantaray, E. Pump, A. Bendjeriou-Sedjerari, V. D'Elia, J. Pelletier, M. Guidotti, R. Psaro, J. M. Basset, *Chem. Soc. Rev.*, 47 (2018) 8403-8437.
- [2] D. Xuereb, R. Raja, *Catal. Sci. Technol.*, 1 (2011) 517.
- [3] F. Quignard, A. Choplin, R. Teissier, *J. Mol. Catal. A: Chem.* 120 (1997) L27.
- [4] E. Gianotti, M. E. Raimondi, L. Marchese, G. Martra, T. Maschmeyer, J. M. Seddon, S. Coluccia, *Catal. Lett.* 76 (2001) 21.
- [5] K. K. Kang, W. S. Ahn, *J. Mol. Catal. A: Chem.* 159 (2000) 403.
- [6] W. Adam, W. Malisch, K. J. Roschmann, C. R. Saha-Moeller, W. A. Schenk, *J. Organomet. Chem.*, 661 (2002) 3.
- [7] A. Held, P. Florczak, *Catal. Today*, 142 (2009) 329.
- [8] C. Perego, R. Millini, *Chem. Soc. Rev.* 42 (9) (2013) 3956–3976.
- [9] O. A. Kholdeeva, N. N. Trukhan, *Russian Chem. Rev.* 75(5) (2006) 411-432.
- [10] *Modern Heterogeneous Oxidation Catalysis* (Ed.: N. Mizuno), Wiley-VCH, Weinheim, 2009.
- [11] J. S. Reddy, P. Liu, A. Sayari, *Appl. Catal. A: Gen.*, 151 (1997) 409.
- [12] Y. Deng, C. Lettmann, W. F. Maier, *Appl. Catal. A: Gen.*, 214 (2001) 31.
- [13] M. Fadhli I. Khedher, J. M. Fraile, *C. R. Chimie* 20 (2017) 827-832.
- [14] N. E. Thornburg, A. B. Thompson, J. M. Notestein, *ACS Catal.*, 5 (2015) 5077–5088.
- [15] X. Li, L. Zhang, H. Gao, Q. Chen, *Russ. J. Phys. Chem. A*, 90 (2016) 1545–1551.
- [16] M. Ziolk, *Catal. Today*, 78 (2003) 47.
- [17] F. Somma, P. Canton, G. Strukul, *J. Catal.* 229 (2005) 490.
- [18] C. Tiozzo, C. Bisio, F. Carniato, A. Gallo, S. L. Scott, R. Psaro, M. Guidotti, *Phys. Chem. Chem. Phys.*, 15 (2013) 13354.
- [19] S. K. Maiti, A. Ramanathan, W. H. Thompson, B. Subramaniam, *Ind. Eng. Chem. Res.* 56 (2017) 1999–2007.
- [20] I. W. C. E. Arends, R. A. Sheldon, *Appl. Catal. A: Gen.*, 212 (2001) 175-187.
- [21] F. Bigi, C. G. Piscopo, G. Predieri, G. Sartori, R. Scotti, R. Zanoni, R. Maggi, *J. Mol. Catal. A: Chem.*, 386 (2014) 108-113.
- [22] Q. Yang, C. Copéret, C. Li, J. M. Basset, *New J. Chem.*, 27 (2003) 319–323.
- [23] C. Aubry, G. Chottard, N. Platzler, J. M. Bregeault, R. Thouvenot, F. Chauveau, C. Huet, H. Ledon, *Inorg. Chem.* 30(23) (1991) 4409-4415.
- [24] M. Faiz Mukhtar Gunam Resul, A. M. López Fernández, A. Rehman, A. P. Harvey, *React. Chem. Eng.*, 3 (2018) 747-756.

- [25] M. Amini, M. M. Haghdoost, M. Bagherzadeh, *Coord. Chem. Rev.*, 268 (2014) 83-100.
- [26] K. Sato, M. Aoki, M. Ogawa, T. Hashimoto, D. Panyella, R. Noyori, *Bull. Chem. Soc. Jpn.*, 70(4) (1997) 905–915.
- [27] D. H. Koo, M. Kim, S. Chang, *Org. Lett.*, 7(22) (2005) 5015-5018.
- [28] K. Kamata, K. Yonehara, Y. Sumida, K. Hirata, S. Nojima, N. Mizuno, *Angew. Chem. Int. Ed.*, 50 (2011) 12062–12066.
- [29] C. Hammond, J. Straus, M. Righettoni, S. E. Pratsinis, I. Hermans, *ACS Catal.*, 3 (2013) 321–327.
- [30] T. R. Amarante, M. M. Antunes, A. A. Valente, F. A. Almeida Paz, M. Pillinger, I. S. Gonçalves, *Inorg. Chem.*, 54 (2015) 9690–9703
- [31] W. L. Dai, J. Ding, Q. Zhu, R. Gao, X. Yang, *Catalysis*, 28 (2016) 1–27.
- [32] N. Maksimchuk, I. Ivanchikova, O. Zalomaeva, Y. Chesalov, A. Shmakov, V. Zaikovskii, O. Kholdeeva, *Catalysts*, 8 (2018) 95.
- [33] C. Y. Cheng, K. J. Lin, M. R. Prasad, S. J. Fu, S. Y. Chang, S. G. Shyu, H. S. Sheu, C. H. Chen, C. H. Chuang, M. T. Lin, *Catal. Commun.* 8 (2007) 1060–1064.
- [34] E. G. Vieira, N. L. Dias Filho, *Mater. Chem. Phys.*, 201 (2017) 262-270.
- [35] H. Chen, N. Li, M. Wang, X. Wang, Q. You, M. Sun, X. Ma, Patent CN 109513458, 2019.
- [36] R. Gao, W. L. Dai, X. Yang, H. Li, K. Fan, *Appl. Catal., A*, 332 (2007) 138.
- [37] M. Jin, Z. Guo, X. Ge, Z. Lv, *React. Kinetics Mech. Catal.* 125 (2018) 1139–1157.
- [38] J. Jarupatrakorn, M. P. Coles, D. Tilley, *Chem. Mater.*, 17 (2005) 1818–1828.
- [39] R. Gao, X. Yang, W. L. Dai, Y. Le, H. Li, K. Fan, *J. Catal.* 256 (2008) 259–267.
- [40] R. Maheswari, M. P. Pachamuthu, A. Ramanathan, B. Subramaniam, *Ind. Eng. Chem. Res.* 53 (2014) 18833–18839.
- [41] A. Ramanathan, R. Maheswari, B. P. Grady, D. S. Moore, D. H. Barich, B. Subramaniam, *Micropor. Mesopor. Mater.*, 175 (2013) 43–49.
- [42] A. Ramanathan, B. Subramaniam, D. Badloe, U. Hanefeld, R. Maheswari, *J. Porous Mater.* 19 (2012) 961–968.
- [43] J. Tang, L. Wang, G. Liu, Y. Liu, Y. Hou, W. Zhang, W. R. Thiel, *J. Mol. Catal. A: Chem.* 313(1-2) (2009) 31–37.
- [44] X. L. Yang, W. L. Dai, H. Chen, J. H. Xu, Y. Cao, H. Li, K. Fan, *Appl. Catal. Gen. A*, 283 (2005) 1-8.
- [45] G. Gelbard, T. Gauducheau, E. Vidal, V. I. Parvulescu, A. Crosman, V. M. Pop, *J. Mol. Catal. A: Chem.* 182–183 (2002) 257–266.
- [46] T. Maschmeyer, F. Rey, G. Sankar, J.M. Thomas, *Nature*, 378 (1995) 159.
- [47] M. Guidotti, N. Ravasio, R. Psaro, G. Ferraris, G. Moretti, *J. Catal.*, 214(2) (2003) 242.

- [48] B. Ravel, M. J. J. Newville, *Synchrotron Radiat.* 8 (2001) 322
- [49] M. Guidotti, B. Lazaro, Deactivation of Molecular Sieves in the Synthesis of Organic Chemicals, in “Deactivation and regeneration of zeolite catalysts”, M. Guisnet, F. Ramoa-Ribeiro (Eds.), Imperial College Press, London, 2011, p. 303-334.
- [50] L. T. Zhuravlev, *Langmuir*, 3 (1987) 316.
- [51] L. J. Burcham, J. Datka, I. E. Wachs, *J. Phys. Chem. B* 103 (1999) 6015.
- [52] J. E. Herrera, J. H. Kwak, J. Z. Hu, Y. Wang, C. H. F. Peden, J. Macht, E. Iglesia, *J. Catal.* 239 (2006) 200–211.
- [53] M. S. Morey, J. D. Bryan, S. Schwarz, G. D. Stucky, *Chem. Mater.*, 12 (2000), 3435–3444.
- [54] E. Gianotti, C. Bisio, L. Marchese, M. Guidotti, N. Ravasio, R. Psaro, S. Coluccia, *J. Phys. Chem. C*, 111 (2007) 5083-5089.
- [55] Z. Zhang, J. Suo, X. Zhang, S. Li, *Appl. Catal. A: Gen.*, 179 (1999) 11-19.
- [56] S. Yamazoe, Y. Hitomi, T. Shishido, T. Tanaka, *J. Phys. Chem. C*, 112 (2008) 6869-6879.
- [57] J. A. Horsley, E. Wachs, J. M. Brown, G. H. Via, F. D. Hardcastle, *J. Phys. Chem.*, 91 (1987) 4014-4020.
- [58] U. Jayarathne, P. Chandrasekaran, A. F. Greene, J. T. Mague, S. DeBeer, K. M. Lancaster, S. Sproules, J. P. Donahue, *Inorg. Chem.*, 53 (2014) 8230–8241.
- [59] S. Yamazoe, Y. Hitomi, T. Shishido, T. Tanaka, *J. Phys. Chem. C*, 112 (2008) 6869-6879.
- [60] V. L. Aksenov, M. V. Koval’chuk, A. Yu. Kuz’min, Yu. Purans, S. I. Tyutyunnikov, *Crystallography Reports*, 51 (2006) 908–935.
- [61] L. Zhenfang, Z. Bisong, *Zeit. Kristall. New Cryst. Struct.*, 223 (2008) 191-193.
- [62] X. Carrier, E. Marceau, H. Carabineiro, V. Rodriguez-Gonzalez, M. Che, *Phys. Chem. Chem. Phys.*, 2009, 11, 7527–7539.
- [63] F. Hilbrig, H. E. Gobel, H. Knozinger, H. Schmelz and B. Lengeler, *J. Phys. Chem.*, 1991, 95, 6973–6978.
- [64] E. I. Ross-Medgaarden, I. E. Wachs, *J. Phys. Chem. C*, 111 (2007) 15089-15099.
- [65] S. Lwin, Y. Li, A. I. Frenkel, I. E. Wachs, *ACS Catal.*, 6 (2016) 3061–3071.
- [66] E. L. Lee, I. E. Wachs, *J. Phys. Chem. C*, 111 (2007) 15089-15099.
- [67] A. Gallo, C. Tiozzo, R. Psaro, F. Carniato, M. Guidotti, *J. Catal.*, 298 (2013) 77.
- [68] C. Cativiela, J.M. Fraile, J.I. Garcia, J.A. Mayoral, *J. Mol. Catal. A* 112 (1996) 259.
- [69] O. A. Kholdeeva, I. D. Ivanchikova, N. V. Maksimchuk, I. Y. Skobelev, *Catal. Today*, 2018, DOI: 10.1016/j.cattod.2018.04.002
- [70] W. Yan, A. Ramanathan, M. Ghanta, B. Subramaniam, *Catal. Sci. Technol.* 2014, 4, 4433.
- [71] A. Köckritz, A. Martin, *Eur. J. Lipid Sci. Technol.* 110 (9) (2008) 812–824.

- [72] M. Guidotti, C. Palumbo, in *Encyclopedia of Inorganic and Bioinorganic Chemistry*, D. A. Atwood (Ed.), John Wiley & Sons, Ltd., Chichester, UK (2016), 1-11.
- [73] E. Poli, R. De Sousa, F. Jerome, Y. Pouilloux, J. M. Clacens, *Catal. Sci. Technol.*, 2 (2012) 910–914.
- [74] Y. Qiao, H. Li, L. Hua, L. Orzechowski, K. Yan, B. Feng, Z. Pan, N. Theyssen, W. Leitner, Z. Hou, *ChemPlusChem*, 77 (2012) 1128 – 1138.
- [75] S. Dworakowska, C. Tiozzo, M. Niemczyk-Wrzeszcz, P. Michorczyk, N. Ravasio, R. Psaro, D. Bogdał, M. Guidotti, *J. Cleaner Prod.*, 166 (2017) 901-909.
- [76] M. Guidotti, R. Psaro, N. Ravasio, M. Sgobba, E. Gianotti, S. Grinberg, *Catal. Lett.*, 122 (2008) 53-56.
- [77] M. Guidotti, E. Gavrilova, A. Galarneau, B. Coq, R. Psaro, N. Ravasio, *Green Chem.*, 13 (2011) 1806-1811.
- [78] L. Vanoye, Z. Eddine Hamami, J. Wang, C. de Bellefon, P. Fongarland, A. Favre-Reguillon, *Eur. J. Lipid Sci. Technol.*, 119 (2017) 1600281.
- [79] S. M. Danov, O. A. Kazantsev, A. L. Esipovich, A. S. Belousov, A. E. Rogozhin, E. A. Kanakov, *Catal. Sci. Technol.*, 7 (2017) 3659–3675.

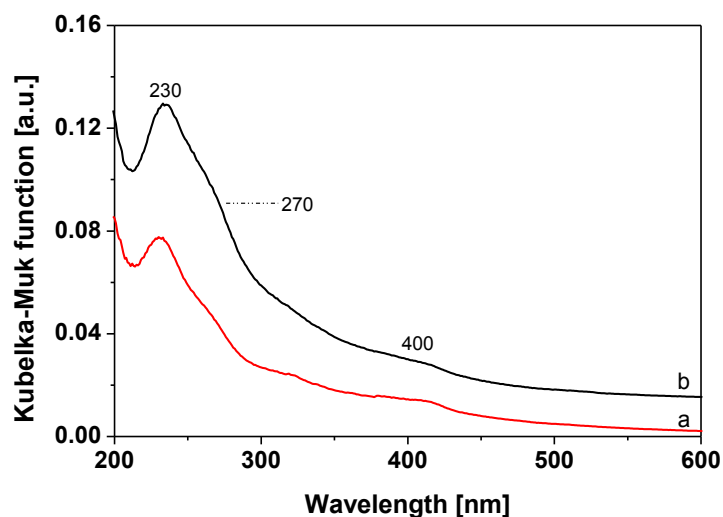


**Figure 1.** DR UV-Vis spectra collected at room temperature of cyclopentadienyl-tungsten species grafted onto  $\text{SiO}_2$  for  $\text{W/SiO}_2\text{-liq}$  (a) and  $\text{W/SiO}_2\text{-DI}$  (b), before calcination, recorded at room temperature.

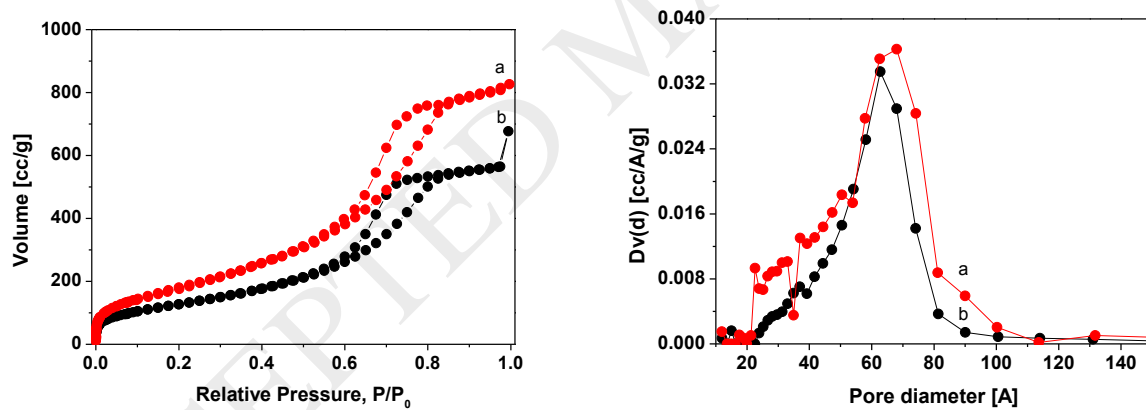


**Figure 2.**  $\text{N}_2$  adsorption-desorption isotherms at 77 K (left) and pores size distribution obtained by NLDFT (right) of  $\text{W/SiO}_2\text{-liq}$  (a) and  $\text{W/SiO}_2\text{-DI}$  (b) samples.

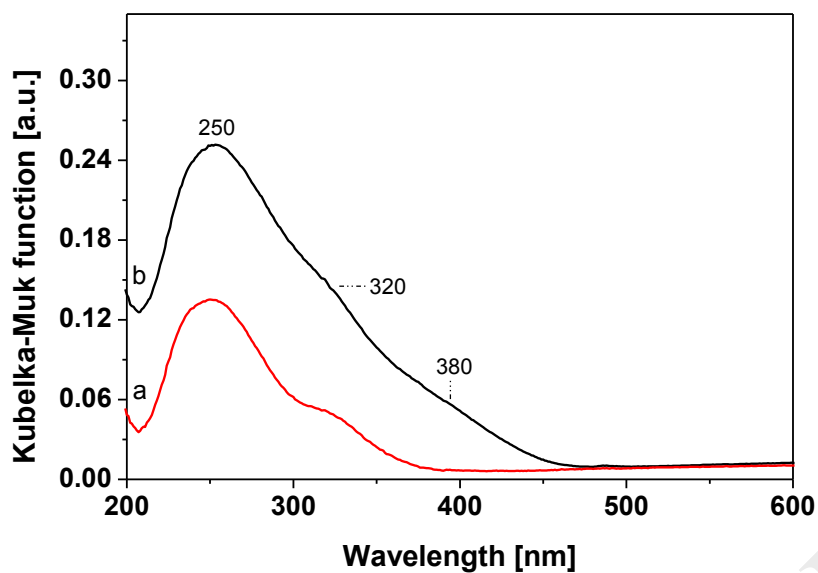


**Figure 3.** DR UV-Vis spectra of W/SiO<sub>2</sub>-liq (a) and W/SiO<sub>2</sub>-DI (b) after calcination, recorded at room temperature.

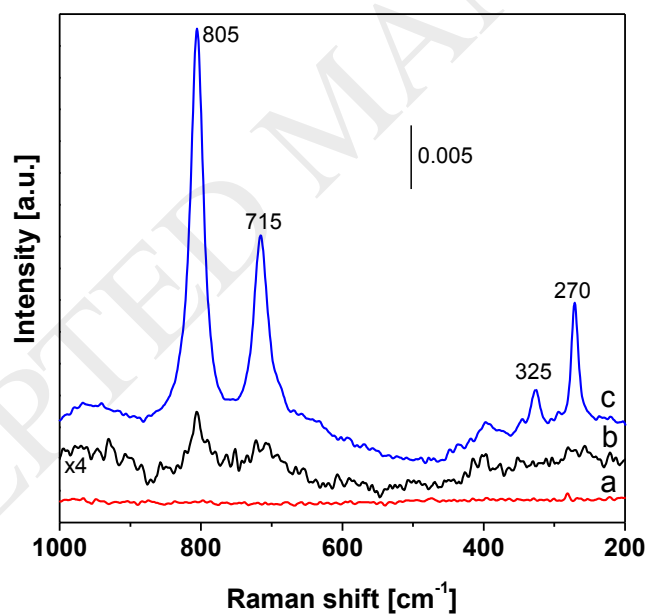


**Figure 4.** Raman spectra of W/SiO<sub>2</sub>-liq (a), W/SiO<sub>2</sub>-DI (b) and commercial WO<sub>3</sub> (c).

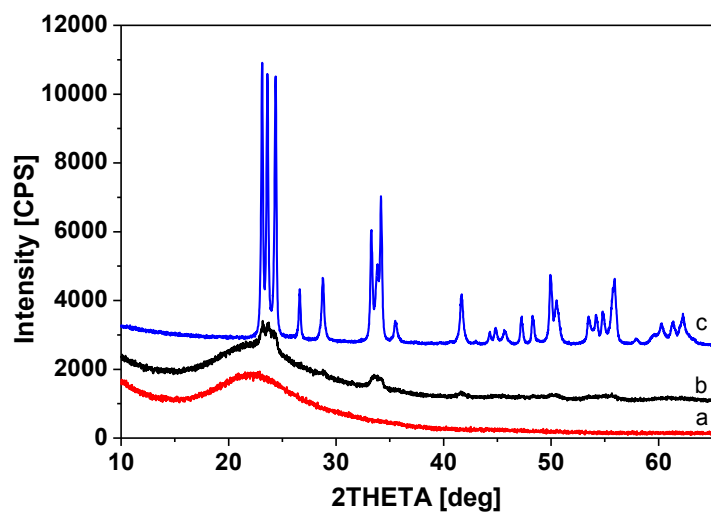


**Figure 5.** X-ray patterns of W/SiO<sub>2</sub>-liq (a), W/SiO<sub>2</sub>-DI (b) and commercial WO<sub>3</sub> (c).

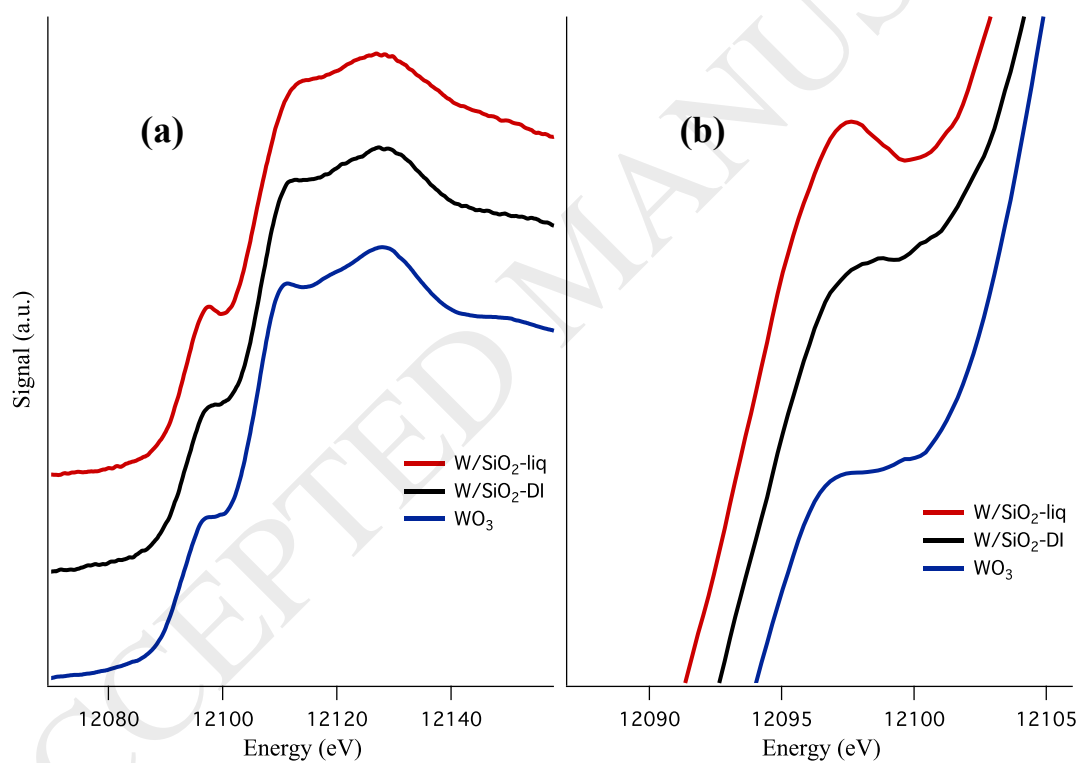


**Figure 6.** W L<sub>1</sub>-edge XANES region. (a) Main edge and (b) pre-edge region.

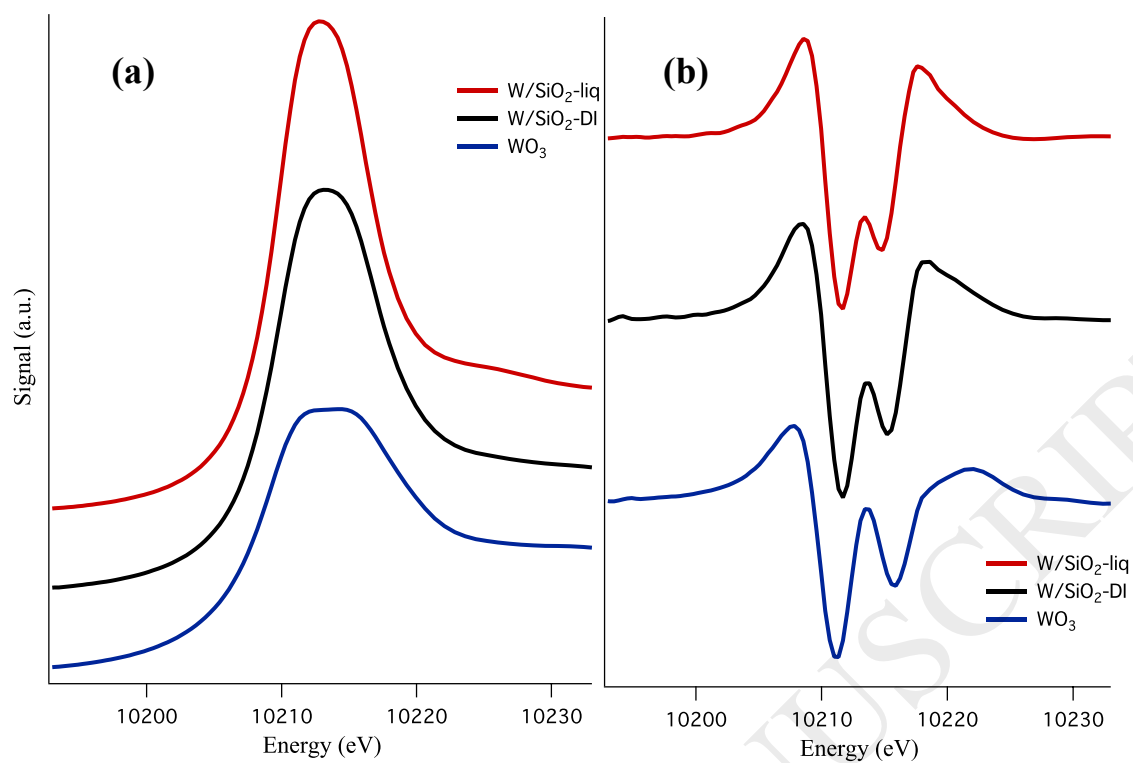


**Figure 7.** W L<sub>3</sub>-edge XANES region. (a) Normalized data and (b) second derivative.

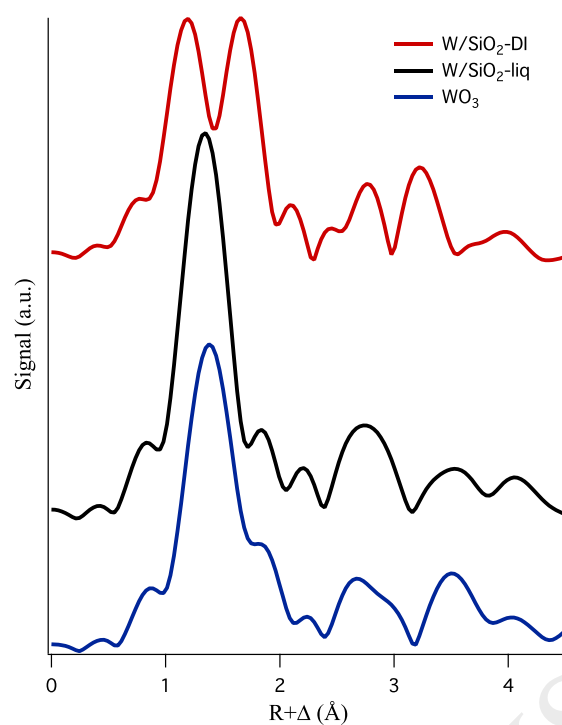


**Figure 8.** Fourier Transform of W  $L_3$ -edge EXAFS data

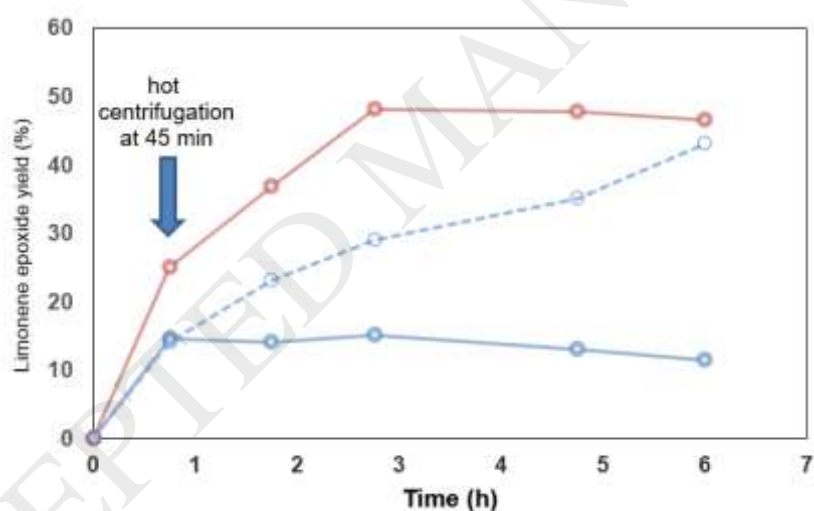


**Figure 9.** Heterogeneity tests for the epoxidation of (*R*)-(+)-limonene. Limonene epoxide yield profile following hot centrifugation, at 45 min, of commercial  $WO_3$  (red curve) and  $W/SiO_2$ -DI (blue solid curve). Epoxide yield profile over  $W/SiO_2$ -DI (without hot centrifugation) is reported for comparison (blue dotted curve). Reaction conditions: 5 mL  $CH_3CN$  solvent; 100 mg catalyst; 1.0 mmol limonene; 2.0 mmol  $H_2O_2$  (aq. 50 wt.%);  $90^\circ C$  oil bath; batch reactor.

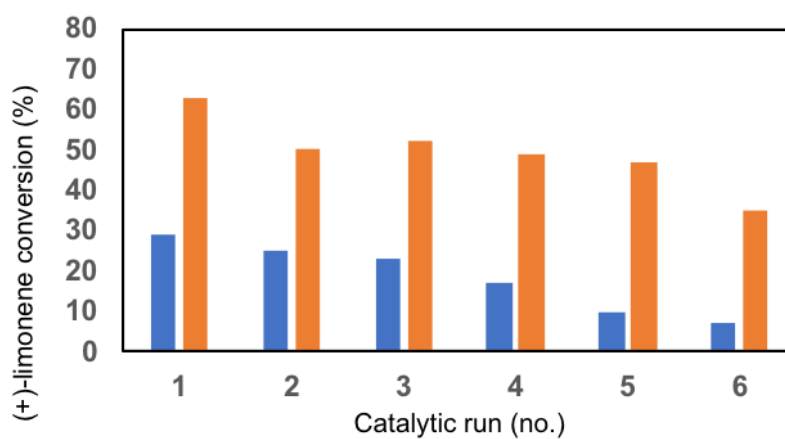


**Figure 10.** Epoxidation of (*R*)- (+)-limonene over W/SiO<sub>2</sub>-DI. Limonene conversion after 1 h (blue bars) and 6 h (orange bars) in consecutive catalytic runs (1 to 6). 10 mL CH<sub>3</sub>CN solvent; 300 mg catalyst; 2.0 mmol (+)-limonene; 4.0 mmol H<sub>2</sub>O<sub>2</sub> (aq. 50 wt.%); 90°C oil bath; batch reactor. The catalyst was washed and activated again at 500°C under dry air prior to each run.

**Table 1.** Metal loading and textural features of the pure support silica and derived tungsten-containing catalysts

Solid	Metal loading (wt.%)	$S_{\text{BET}}$ ( $\text{m}^2 \text{g}^{-1}$ )	PV ( $\text{cm}^3 \text{g}^{-1}$ )
$\text{SiO}_2$	-	605	1.11
W/ $\text{SiO}_2$ -liq	1.18	603	1.38
W/ $\text{SiO}_2$ -DI	1.70	465	1.10

**Table 2.** Catalytic performance of tungsten-silica catalysts in the liquid-phase epoxidation of (*R*)-(+)-limonene

Catalyst	$C^a$ 1h (%)	$Y^b$ 1h (%)	C 6h (%)	Y 6h (%)	<i>endo:exo</i> ratio <sup>c</sup>	<i>cis:trans</i> ratio <sup>d</sup>	$SA^e$ ( $\text{h}^{-1}$ )
$\text{WO}_3^f$	47	38	80	54	80:20	79:21	1.1
$\text{WO}_3^g$	21	17	76	45	81:19	74:26	0.5
W/ $\text{SiO}_2$ -liq	18	11	55	31	77:23	80:20	28
W/ $\text{SiO}_2$ -DI	20	15	68	43	83:17	80:20	31
W/ $\text{SiO}_2$ -DI <sup>h</sup>	21	n.d.	55	2	n.d. <sup>i</sup>	n.d.	33

Conditions: 5 mL  $\text{CH}_3\text{CN}$  solvent; 100 mg catalyst; 1.0 mmol (+)-limonene; 2.0 mmol  $\text{H}_2\text{O}_2$  (aq. 50 wt.%); 90°C oil bath; batch reactor. a: limonene conversion; b: yield to limonene epoxides (*endo-cis* + *exo-trans* + *exo*); c: endocyclic to exocyclic limonene epoxide molar ratio after 6 h; d: *cis* to *trans* endocyclic limonene epoxide molar ratio after 6 h; e: specific activity ( $[\text{mol}_{\text{converted alkene}}] [\text{mol}_W \text{h}]^{-1}$ ) after 1h; f: commercial  $\text{WO}_3$  catalyst pretreated at 120°C in air for 1 h and in vacuo for 1 h prior to use; g: commercial  $\text{WO}_3$  catalyst pretreated at 500°C in dry air for 1 h prior to use; h: 1.1 mmol *tert*-butylhydroperoxide, TBHP, as oxidant; i: non-detectable.

**Table 3.** Catalytic performance of tungsten-silica catalysts in the liquid-phase epoxidation of methyl oleate

Catalyst	H <sub>2</sub> O <sub>2</sub> / oleate ratio	C <sup>a</sup> 1h (%)	Y <sup>b</sup> 1h (%)	C 6h (%)	Y 6h (%)	<i>cis:trans</i> ratio <sup>c</sup>	SA <sup>d</sup> (h <sup>-1</sup> )
W/SiO <sub>2</sub> -liq	2 : 1	13	9	37	25	63:37	20
W/SiO <sub>2</sub> -liq	4 : 1	20	11	43	30	58:42	31
W/SiO <sub>2</sub> -DI	2 : 1	10	5	43	34	85:15	11
W/SiO <sub>2</sub> -DI	4 : 1	16	12	65	51	67:33	17

Conditions: 5 mL CH<sub>3</sub>CN solvent; 100 mg catalyst; 1.0 mmol methyl oleate; H<sub>2</sub>O<sub>2</sub> (aq. 50 wt.%); 90°C oil bath; batch reactor. a: methyl oleate conversion; b: yield to methyl epoxystearate; c: *cis* to *trans* methyl epoxystearate molar ratio after 6 h; d: specific activity ( $[\text{mol}_{\text{converted oleate}}] [\text{mol}_{\text{W}} \text{h}^{-1}]$ ) after 1h.